BB

GSI-95-16
PREPRINT
FEBRUAR 1995

COLLECTIVE FLOW OF PIONS IN RELATIVISTIC HEAVY-ION COLLISIONS

V.N. RUSSKIKH, Yu.B. IVANOV

Gesellschaft für Schwerionenforschung mbH
Postfach 11 05 52 D-64220 Darmstadt Germany

Collective Flow of Pions in Relativistic Heavy-Ion Collisions

V.N. Russkikh* and Yu.B. Ivanov*

Gesellschaft für Schwerionenforschung (GSI), Postfach 110552, D-64220 Darmstadt, Germany

February 22, 1995

Abstract

The transverse-momentum distributions of pions in the Au(1 GeV/nucleon) + Au collisions are analyzed. The calculations are carried out within relativistic mean-field one- and two-fluid models. The rapidity distributions of the mean transverse momentum of pions are found to be fairly sensitive to the nuclear equation of state and, especially, to the stopping power. It is shown that the collective flow of pions in the reaction plane always correlates with the "hot" flow of nucleons (i.e. those emitted from hot regions of nuclear system), while not always, with the total nucleon flow. This "hot" nucleon flow can be experimentally singled out by selecting nucleons with sufficiently high transverse momenta. We predict that the "hot" nucleon flow selected in this way will always correlate with the pion flow. Available experimental data on transverse-momentum spectra of pions are compared with calculations employing various equations of state and stopping power.

* Permanent address: Kurchatov Institute, Moscow 123182, Russia
e-mail: russ@kiae.su and ivan@kiae.su

The equation of state (EOS) of dense and hot nuclear matter and its transport properties still remain the main objectives of the heavy-ion researches. A rather long experience of these experimental and theoretical investigations indicates that the properties of nuclear matter cannot be deduced from any single observable alone. To reach this goal, one should fit simultaneously all the observables being sensitive to the nuclear EOS and transport properties. A number of global baryon observables, such as the bounce-off and squeeze-out [1], has been found to be fairly sensitive to these characteristics. Pion observables provide additional information for such analysis. Without being restricted by the particle-number conservation, pions are generally believed to be more sensitive to the nuclear EOS and transport properties. This inspired 4π measurements of pion yield in the streamer-chamber experiment at the Bevalac [2, 3]. Indeed, while the sensitivity of pion yields and spectra to the EOS (more precisely, to the compressibility of the nuclear matter [4, 5]) proves to be not very high [4, 5, 6, 7], they are quite sensitive to the momentum dependence of nuclear forces and nuclear stopping power [4, 5, 8].

Presently, new experimental setups at the GSI/SIS heavy-ion accelerator (FOPI, KaoS and TAPS [9, 10, 11]) provide us with more precise and complete data on pion production. In particular, these data allow us to analyze the collective flow of pions produced in heavy-ion collisions. In this paper we study global pion observables, such as the in-plane distribution of the transverse momentum $p_x(y)$ [12], discuss their relation to the corresponding nucleon observables and demonstrate their sensitivity to the nuclear EOS and stopping power (SP). We also compare transverse-momentum spectra of pions with available experimental data. The treatment is based on the calculations of Au(1 GeV/nucleon) + Au collisions within relativistic mean-field one- and two-fluid models (RMF-1FM [5] and RMF-2FM [13, 14], correspondingly). Similar calculations but within the IQMD model have been recently performed in refs. [15, 16, 17], where the sensitivity of the pion global observables to the EOS were examined. In principle, the study of the SP is also of great interest by itself, since hadron cross sections in the nuclear medium are not necessarily vacuum ones. They can differ from the latter due to the medium polarization [19]. The SP can also be modified by multinucleon interactions [20, 21]. Calculations within the one- and two-fluid models allow us to test the sensitivity to the SP, since the one-fluid model is a limiting case of the two-fluid one with infinite SP.

The RMF-2FM (see refs. [13, 14] for details) assumes that the leading nonequilibrium in nuclear collisions occurs due to a finite stopping power of nuclear matter. Hence, it treats two interacting hadronic fluids (originally associated with the projectile and target nucleons) moving in self-consistent mean σ and ω fields [22, 23], which correspond to a certain EOS in equilibrium. The input of this model consists of mean-field parameters and cross-sections, i.e. it is just the same as that in the mean-field kinetic models. The pion production is treated in the RMF-2FM via the Δ resonance excitation. The pions and deltas are assumed to be in local thermal equil'' rium within each of two hadronic fluids. They evolve together with these fluids till the moment of the freeze-out, at which the disintegration of a locally frozen-out fluid element occurs. For the mean σ and ω fields the nonlinear parametrizations of ref. [24] are used (see table 1).

Table 1. Properties of the mean-field parametrizations due to ref. [24]: the saturation nuclear density (n_0), the binding energy at n_0 (ε_B), the compressibility (K_0) and the nucleon effective mass (M^*_{N0}) for the ground state of nuclear matter.

EOS	n_0, fm^{-3}	ε_B, MeV	K_0, MeV	M^*_{N0}/M_N
Stiff	0.15	16.0	400	0.65
Soft	0.15	16.0	210	0.85

These parametrizations reproduce the ground state of nuclear matter but yield different compressibilities and effective nucleon masses in the ground state. Hence, they result in the stiff and soft EOS's. The vacuum nucleon-nucleon cross sections according to the Cugnon parametrization [25] are used in the present calculation. To test the sensitivity to the SP, we also perform the calculations within the RMF-1FM [5]. Contrary to the RMF-2FM, the RMF-1FM assumes an immediate equilibration of two flows and, hence, gives the complete mutual stopping. The isotopic content of the species (N, Δ and π) produced in the collision is calculated in the spirit of the thermodynamical approach [26] (cf. Appendix).

To demonstrate the sensitivity of inclusive pion data to the EOS and SP, in fig. 1 we present the comparison of new data of the TAPS collaboration [29] on the transverse-momentum spectrum of neutral pions with calculations within the RMF-1FM and RMF-2FM. As seen, the stiff RMF-2FM is evidently wo: ' at the data reproduction. Nevertheless, below we present predictions of this version of the model in order to demonstrate the dependence on the EOS and SP. All other calculations basically underestimate the data too. The underestimation of the low-energy pion yield is a long-standing problem of most of the transport theories (see discussion in [28]). Probably, it occurs due to medium modification of soft pions [30]. While, the high-energy tail of the pion spectra is usually better reproduced [14]. However, the single sample of data is not enough to judge on the preference this or that EOS and SP. As one can see in fig. 2, the same two-fluid calculation (with soft EOS) almost perfectly reproduces the data of the KaoS collaboration [27] o·· the positive pion production in the same collisions. This spectrum at the laboratory angle $\theta_{lab} = 44°$ roughly corresponds to the p_t-distribution at the midrapidity, i.e. to that presented in fig. 1. A slight underestimation in the high-energy range $0.7 \lesssim p_{lab} \lesssim 1$ GeV/c (by the soft RMF-2FM) can be naturally associated with the contribution of decays of heavier resonances. The work on taking into account these heavy resonances is in progress now. To be consistent, in fig. 3 presented are our predictions for the forthcoming data of the FOPI collaboration on the π^--production. Here and below, the "normalized" rapidity is $y_{cm}^{(0)} = y_{cm}/y_{cm}^{(proj.)}$, where y_{cm} is the pion rapidity in the center of mass of colliding nuclei and $y_{cm}^{(proj.)} = 0.68$ is the center-of-mass rapidity of the projectile nucleus. It is worthy of mentioning that the calculations with soft EOS are, as a rule, the best at reproduction of various data on nuclear collisions [14].

Fig. 4 presents predictions of the models for the rapidity distributions of the mean transverse momentum of negative pions in the reaction plane due to the transverse-momentum analysis of Danielewicz and Odyniec [12]. Here, the mean transverse momentum $\langle p_x(y) \rangle$ is divided by the pion mass (m_π). As seen, the variation of the EOS results in a noticeable quantitative change of the $p_x(y)$ distribution. At the stiff EOS the p_x distributions are considerably steeper than those at the soft one. The variation of the SP brings about even the qualitative change of the $p_x(y)$ distribution. In the RMF-1FM the pion transverse flow always correlates with the nucleon ones, while at the SP, determined by the Cugnon cross sections, the pion transverse flow disappears at a certain intermediate impact parameter (b) and at larger b it starts to anticorrelate with the nucleon flow. This qualitative change of the flow pattern is manifestly exhibited by a more global observable

$$p_x^{dir} = \frac{1}{N_\pi} \sum_{i=1}^{N_\pi} p_x^i \, sign(y_i - y_{cm}) \qquad (1)$$

displayed in fig. 5. Here the sum runs over pions, N_π is the number of pions in the event, and y_{cm} means the rapidity of the center of mass of two colliding nuclei. Both fig. 4 and fig. 5 show that the one-fluid model always predicts the normal behavior of the pion flow (i.e. the positive slope of $\langle p_x \rangle$ at $y_{cm} = 0$), while the two-fluid one yields inverse pion flow for impact parameters greater than 4 fm. It means that such inverse flow of pions originates due to the partial transparency or finite SP of nuclear matter. Hence, the pion flow is sensitive to the nucleon-nucleon cross sections in the medium, which determine the

SP.

A similar effect of the proton-pion anticorrelation has been observed in the asymmetric Ne(0.8 GeV/nucleon) + Pb collisions by the DIOGENE collaboration [31]. In the symmetric system Au + Au, this effect proves to be more spectacular. The DIOGENE data [31] were analyzed within IQMD [15] and BUU [28, 32] models, where this anticorrelation effect was explained by peculiarities of the pion scattering on spectator parts of colliding nuclei [15] and, alternatively, by the pion absorption in spectators [28, 32]. Here, we suggest a more macroscopic interpretation of this effect which does not reject the above microscopic explanations.

In fact, the nucleon collective flow in the reaction plane is characterized by the whole distribution of temperatures and velocities. It includes a relatively cold flow of nuclear matter exercised the bounce-off, as well as the flow of hot participant nucleons undergone the expansion. The flow pattern of this latter system essentially depends on the EOS and especially strongly on the SP. The dependence on the SP is illustrated in fig. 6, where the evolution of the temperature in the reaction plane is displayed for the Au(1 GeV/nucleon) + Au collision at the impact parameter $b = 6$ fm within the RMF-1FM (the left panel) and RMF-2FM (the right panel) employing the soft EOS. These illustrative calculations were performed without freezing-out. The fluid-dynamical evolution was followed till the very low densities. This is the reason for the numerical fragmentation of the matter occurred at $t = 31.06$ fm/c within the RMF-2FM. Since within the RMF-2FM the interpenetration of two fluids essentially occurs at the initial stage of the collision, in the figure we display the density-weighted temperature defined as

$$T = \frac{N^{(p)}T^{(p)} + N^{(t)}T^{(t)}}{N^{(p)} + N^{(t)}}. \tag{2}$$

where $T^{(p)}$ and $T^{(t)}$ are the temperatures of the "projectile" and "target" fluids, respectively, while $N^{(p)}$ and $N^{(t)}$ are the corresponding baryon densities in the c.m. frame of colliding nuclei. The hot zone is spatially located at the center of mass of two colliding nuclei. Within the one-fluid model (i.e. at the infinite SP), the distribution of collective velocities in this zone is elongated into directions of the projectile and target spectators undergone the bounce-off. Note that these spectators are only relatively cold, decaying they produce the relatively cold bounce-off flow. The further expansion of the hot zone mainly proceeds along this direction, resulting in the further enhancement of the bounce-off flow. Hence, the flow of participants is similar to the bounce-off one. In the case of the partial transparency (i.e. within the two-fluid model) the hot central region expands more isotropically as compared with the one-fluid case. It is clearly seen from comparison of the corresponding plots at the instant $t = 15.53$ fm/c. However, this almost isotropic expansion is partially screened by the spectators, which experience considerably weaker bounce-off. This forces the hot participant matter to expand predominantly into sideward directions opposite to those of the bounce-off, as it is seen already at the next instant $t = 20.7$ fm/c. Precisely this sideward expansion changes the one-fluid flow pattern and brings about the anticorrelation between the hot-participant flow and the bounce-off one. In terms of microscopic models, this collective sideward expansion can be associated with either the reflection or shadowing of participant particles from/by the spectator matter. Macroscopically, this effect may be called as "collective shadowing".

In this speculation we have not distinguished between pions and nucleons from the hot zone. Indeed, our observation is that the hot part of the in-plane nucleon flow always correlates with the corresponding pionic flow. This is illustrated in fig. 7, where the p_x distributions for all the protons ($p_t > 50$ MeV/c), only "hot" protons ($T > 60$ MeV) and negative pions (π^-) are displayed. These distributions are calculated within the soft RMF-2FM at $b = 6$ fm impact parameter. To construct the distribution of the "hot" protons, only protons from those regions of the nuclear system, which had temperatures $T > 60$ MeV at the freeze-out moment, were taken into account. Indeed, one can see that the hot-proton flow correlates with the pionic one, unlike the flow of all the protons. Moreover, the fact that the mean velocities ($v_x = \langle p_x \rangle / m$) of pions and "hot" protons are almost equal in the midrapidity region indicates that both the pions and "hot" nucleons originate from the same collective flow. Thus, studying global observables of pions, we gain information on the collective flow of the hot nuclear matter. The collective flow of hot nucleons can also be extracted by a direct semi-experimental selection. In fig. 7, $\langle p_x \rangle$ of protons, possessing high transverse momenta $p_t > 1$ GeV/c, is displayed. Such protons are predominantly radiated by hot regions of the nuclear system. As seen, the collective flow of thus selected protons correlates with the pionic flow.

In conclusion, we have performed calculations of inclusive transverse-momentum spectra of pions and confronted them to available experimental data from the GSI/SIS accelerator. The calculations were performed within relativistic mean-field one- and two-fluid models. It has been demonstrated the RMF-2FM with soft EOS fairly well reproduces the π^+ data, while the description of the π^0 data is far from being perfect. We have also considered rapidity distributions of the mean transverse momentum of pions in the reaction plane in collisions Au(1 GeV/nucleon) + Au. Such kind of data will be soon available from the 4π experiments at the GSI. The sensitivity of these distributions to the nuclear EOS and especially to the SP has been demonstrated. It has been shown that the pionic collective flow in the reaction plane correlates with the corresponding flow of nucleons emitted from hot regions of nuclear system, while not always with the total nucleon flow. The one-fluid model always predicts the correlation between the pionic flow and the total nucleon one. The inverse behavior of the pion flow results from the partial transparency of nuclei, and due to this fact the pion flow may serve as a tool for investigation of the in-medium nucleon-nucleon cross sections. This "hot" nucleon flow can be experimentally singled out by selecting nucleons with sufficiently high transverse momenta. Thus, in-plane transverse-momentum distributions of pions simultaneously provide us with information on the collective flow of hot participant nucleons. All this makes the pionic transverse-momentum distributions to be highly useful for deducing the EOS and SP of nuclear matter from forthcoming experimental data.

Acknowledgments. We are grateful to P. Senger and R. S. Simon for providing us with files of the experimental data. This work is supported in part by International Science Foundation under the grant ISF-N8Z000, by the International Association for the Promotion of Cooperation with Scientists from the Independent States of the Former Soviet Union under the grant INTAS-94-3405, and by BMFT. We highly appreciate the hospitality and support rendered to us at the GSI, where the final part of this work was performed.

Appendix

If the colliding nuclei are isotopically asymmetric ($Z/A < 1/2$), the numbers of different species Δ^{++}, Δ^{+}, Δ^{0}, Δ^{-}, π^{+}, π^{0} and π^{-} produced in the collision are also asymmetric. This asymmetry is calculated in the spirit of thermodynamic approach of Kapusta [26]. This way of calculation is more consistent with our RMF-1FM and RMF-2FM than that described in ref. [14].

The chemical potentials of all these species are related to each other as follows

$$\begin{aligned} \mu_\Delta^{++} - \mu_\Delta^{+} &= \mu_\Delta^{+} - \mu_\Delta^{0} = \mu_\Delta^{0} - \mu_\Delta^{-} = \Delta\mu, \\ \mu_\pi^{+} - \mu_\pi^{0} &= \mu_\pi^{0} - \mu_\pi^{-} = \Delta\mu. \end{aligned} \tag{A.1}$$

where

$$\Delta\mu = \mu_p - \mu_n$$

is the difference between proton and neutron chemical potentials. These relations provide explicit conservation of electric charge. If we take the Maxwell distribution functions (what is reasonable for the freeze-out stage) for all the species, we obtain for the numbers of different species (N_i) the following relations

$$
\begin{aligned}
N_p/N_n &= x, \\
N_\Delta^{++}/N_\Delta^{+}/N_\Delta^{0}/N_\Delta^{-} &= x^2/x/1/x^{-1}, \\
N_\pi^{+}/N_\pi^{0}/N_\pi^{-} &= x/1/x^{-1},
\end{aligned}
\tag{A.2}
$$

where

$$x = \exp(\Delta\mu/T).$$

Now we can write the set of equations for determining x

$$
\begin{aligned}
N_n(x+1) &= N_N, \\
N_\Delta^0(x^2+x+1+x^{-1}) &= N_\Delta, \\
N_\pi^0(x+1+x^{-1}) &= N_\pi, \\
xN_n + (2x^2+x-x^{-1})N_\Delta^0 + (x-x^{-1})N_\pi^0 &= \frac{Z}{A}(N_N+N_\Delta),
\end{aligned}
\tag{A.3}
$$

where N_N, N_Δ and N_π are the total numbers of nucleons, deltas and pions, correspondingly. The last equation expresses the conservation of the isospin (or the electric charge), Z and A are the total number of protons and nucleons in the initial nucleus, correspondingly. The N_N, N_Δ and N_π numbers are known from the solution of the fluid-dynamics equations. By excluding N_n, N_Δ^0 and N_π^0 from these equations, we get the single equation for x

$$\frac{x}{x+1}N_N + \frac{2x^2+x-x^{-1}}{x^2+x+1+x^{-1}}N_\Delta + \frac{x-x^{-1}}{x+1+x^{-1}}N_\pi = \frac{Z}{A}(N_N+N_\Delta). \tag{A.4}$$

By solving this equation, we determine x and, thus, all the required quantities. Eq. (A.4) is solved locally for each fluid element. When all the deltas decay, they give the contribution to pion numbers

$$
\begin{aligned}
N_{\Delta\to\pi}^{-} &= N_\Delta^{-} + \frac{1}{3}N_\Delta^{0}, \\
N_{\Delta\to\pi}^{0} &= \frac{2}{3}(N_\Delta^{0} + N_\Delta^{+}), \\
N_{\Delta\to\pi}^{+} &= N_\Delta^{++} + \frac{1}{3}N_\Delta^{+},
\end{aligned}
\tag{A.5}
$$

which are calculated in terms of branching ratios of the $\Delta \to \pi N$ decay. These decays also contribute to the nucleon numbers

$$
\begin{aligned}
N_{\Delta\to n} &= N_\Delta^{-} + \frac{2}{3}N_\Delta^{0} + \frac{1}{3}N_\Delta^{+}, \\
N_{\Delta\to p} &= \frac{1}{3}N_\Delta^{0} + \frac{2}{3}N_\Delta^{+} + N_\Delta^{++}.
\end{aligned}
\tag{A.6}
$$

Note that the proportion between Δ-induced pion numbers $N^+_{\Delta\to\pi}$, $N^0_{\Delta\to\pi}$ and $N^-_{\Delta\to\pi}$ is generally different from that for thermal pions. The same holds for Δ-induced nucleons.

References

[1] H. Stöcker and W. Greiner, Phys. Rep. **137** (1986) 277.

[2] A. Sandoval et al., Phys. Rev. Lett. **45** (1980) 874; R. Stock et al., Phys. Rev. Lett. **49** (1982) 1236; J. Harris et al., Phys. Lett. **B153** (1985) 377.

[3] R. Stock, Phys. Rep. 135 (1986) 261.

[4] M. Cubero, M. Schönhofen, H. Feldmeier and W. Nörenberg, Phys. Lett. **201B** (1988) 11; M. Schönhofen, M. Cubero, M. Gering, M. Sambataro, H. Feldmeier and W. Nörenberg, Nucl. Phys. **A504** (1989) 875.

[5] V. N. Russkikh, Sov. J. Nucl. Phys. **53** (1991) 1037; V. N. Russkikh and Yu. B.Ivanov, Nucl. Phys. **A543** (1992) 751

[6] H. Kruse, B. V. Jacak and H. Stöcker, Phys. Rev. Lett. **54** (1985) 289.

[7] P. Danielewicz and G. F. Bertsch, Nucl. Phys. **A533** (1991) 712.

[8] Yu. B. Ivanov and V. N. Russkikh, Nucl. Phys. **A580** (1994) 614.

[9] N. Herrmann and the FOPI collaboration, Nucl. Phys. **A553** (1993) 739c.

[10] D. Brill and the KaoS collaboration, Phys. Rev. Lett. **71** (1993) 336.

[11] L. Venema and the TAPS collaboration, Phys. Rev. Lett. **71** (1993) 835.

[12] P. Danielewicz and G. Odyniec, Phys. Lett. **157B** (1985) 146.

[13] Yu.B. Ivanov, V.N. Russkikh, M. Schönhofen, M. Cubero, B.L. Friman and W. Nörenberg, Z. Phys. **A340** (1991) 385

[14] V.N. Russkikh, Yu.B. Ivanov, Yu.E. Pokrovsky and P.A. Henning, Nucl. Phys. **A572** (1994) 749.

[15] S. A. Bass, C. Hartnack, R. Mattiello, H. Stöcker and W. Greiner, Phys. Lett. **302B** (1993) 381.

[16] S. A. Bass, C. Hartnack, H. Stöcker and W. Greiner, Phys. Rev. Lett. **71** (1993) 1144.

[17] S. A. Bass, C. Hartnack, H. Stöcker and W. Greiner, Preprint GSI-94-14 (1994).

[18] S. A. Bass, C. Hartnack, H. Stöcker and W. Greiner, Preprint GSI-95-07 (1995).

[19] B. ter Haar and R. Malfliet, Phys. Rev. **C36** (1987) 1611;
F. de Jong, B. ter Haar and R. Malfliet, Phys. Lett. **220B** (1989) 533.

[20] A. Bonasera and F. Gulminelli, Phys. Lett. **259B** (1991) 399, **275B** (1992) 24.

[21] G. Batko, J. Randrup and T. Vetter, Nucl. Phys. **A536** (1992) 786.

[22] J. D. Walecka, Ann. of Phys., **83** (1974) 491.

[23] B. D. Serot and J. D. Walecka, *The Relativistic Nuclear Many-Body Problem*, Adv. Nucl. Sci. **16** (1986) 1.

[24] B. Waldhauser, J. A. Maruhn, H. Stöcker and W. Greiner, Phys. Rev. **C38** (1988) 1003.

[25] J. Cugnon, Phys. Rev. **C22** (1980) 1885.

[26] J. I. Kapusta, Phys. Rev. **C16** (1977) 1493.

[27] D. Miskowiec and the KaoS collaboration, Phys. Rev. Lett. **72** (1994) 3650.

[28] P. Danielewicz, Preprint of the Michigan State University, MSUCL-946 (1994).

[29] O. Schwalb et al., Phys. Lett. **321B** (1994) 20.

[30] D. N. Voskresensky, Nucl. Phys. **A555** (1992) 293.

[31] J. Gosset and the DIOGENE collaboration, Phys. Rev. Lett. **62** (1989) 1251.

[32] B. A. Li, W. Bauer and G. F. Bertsch, Phys. Rev. **C44** (1991) 2095.

Figure captions

Fig. 1. Differential cross section of neutral pions as a function of the transverse momentum measured at the midrapidity (i.e within the laboratory rapidity interval $0.52 < y_{lab} < 0.84$) in Au(1 GeV/nucleon) + Au collisions as compared with calculations within the RMF-1FM and RMF-2FM. Data are from ref. [29].

Fig. 2. Double differential cross section for positive pions as a function of the laboratory momentum measured at $40° < \theta_{lab} < 48°$ in Au(1 GeV/nucleon) + Au collisions as compared with calculations within the RMF-1FM and RMF-2FM. Data are from ref. [27].

Fig. 3. Predictions for the double differential cross section of negative pions as a function of the transverse momentum measured at midrapidity in Au(1 GeV/nucleon) + Au collisions. The "normalized" rapidity is $y_{cm}^{(0)} = y_{cm}/y_{cm}^{(proj.)}$, where y_{cm} is the pion rapidity in the center of mass of colliding nuclei and $y_{cm}^{(proj.)} = 0.68$ is the rapidity of the projectile nucleus in the center of mass of colliding nuclei.

Fig. 4. Rapidity distributions of the mean transverse momentum of negative pions [divided by the pion mass (m_π)] in Au(1 GeV/nucleon) + Au collisions at various impact parameters. Only pions with total transverse momenta in the range $0.2 < p_t < 0.6$ GeV/c are taken into account in these distributions. The "normalized" rapidity $y_{cm}^{(0)}$ is the same as in fig. 3.

Fig. 5. Directed transverse momentum per pion as a function of the impact parameter in Au(1 GeV/nucleon) + Au collisions.

Fig. 6. Temperature contour plots (in the reaction plane) for the Au(1 GeV/nucleon) + Au collision at the impact parameter $b = 6$ fm calculated within the RMF-1FM (the left panel) and RMF-2FM (the right panel) employing the soft EOS. The spatial axis z corresponds the beam one, while the x-axis is that transverse to the beam axis. The plots are displayed at the time instants indicated in the upper right corners of each frame. Dotted lines show the boundary of the region occupied by nuclear matter. The temperatures inside the outer solid contour are $T > 20$ MeV, inside the outer dashed contour are $T > 40$ MeV, inside the inner solid contour are $T > 60$ MeV, and inside the inner dashed contour are $T > 80$ MeV. The collective velocities of the nuclear matter are indicated by

arrows. The arrows start at the position of the fluid element they belong to. The direction and size of the arrow correspond to the direction and magnitude of the corresponding velocity.

Fig. 7. Rapidity distributions of the mean transverse momentum divided by the proper mass [either the pion mass (m_π) or the nucleon one (M_N)] of negative pions (π^-), all the protons ($p_t > 50$ MeV/c), theoretically selected hot protons ($T > 60$ MeV), and semi-experimentally selected hot protons ($p_t > 1$ GeV/c). The "normalized" rapidity$y_{cm}^{(0)}$ and the restriction on the total pion transverse momentum are the same as in fig. 3. The distributions are calculated within the soft RMF-2FM for Au(1 GeV/nucleon) + Au collision at the impact parameter $b = 6$ fm.

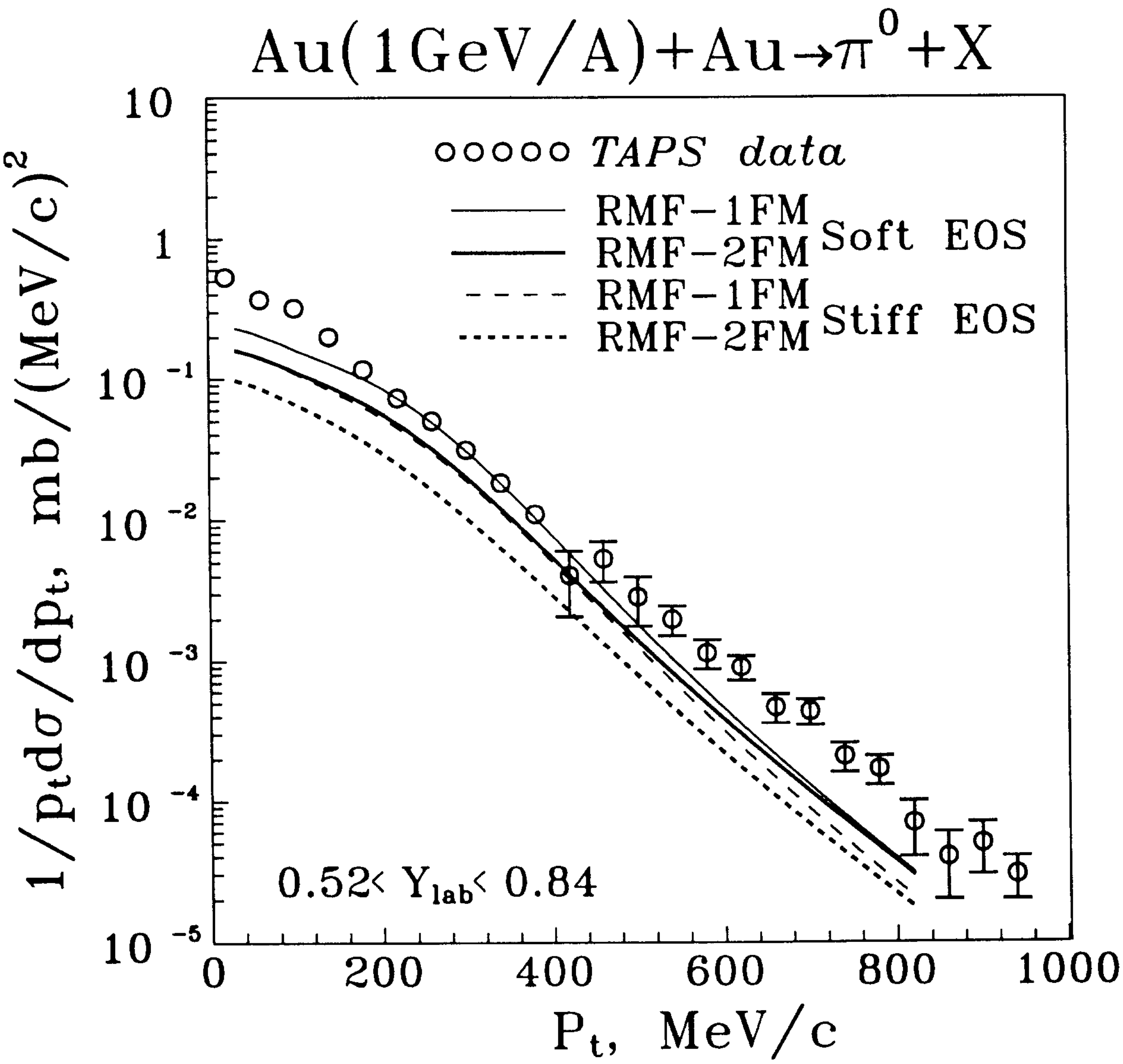
Au(1GeV/A)+Au→π⁰+X
○○○○○ TAPS data
RMF−1FM
RMF−2FM
Soft EOS
RMF−1FM
RMF−2FM
Stiff EOS
0.52< Y_lab< 0.84
1/p_t dσ/dp_t, mb/(MeV/c)^2
P_t, MeV/c
10
1
10^-1
10^-2
10^-3
10^-4
10^-5
0
200
400
600
800
1000

Fig. 1.

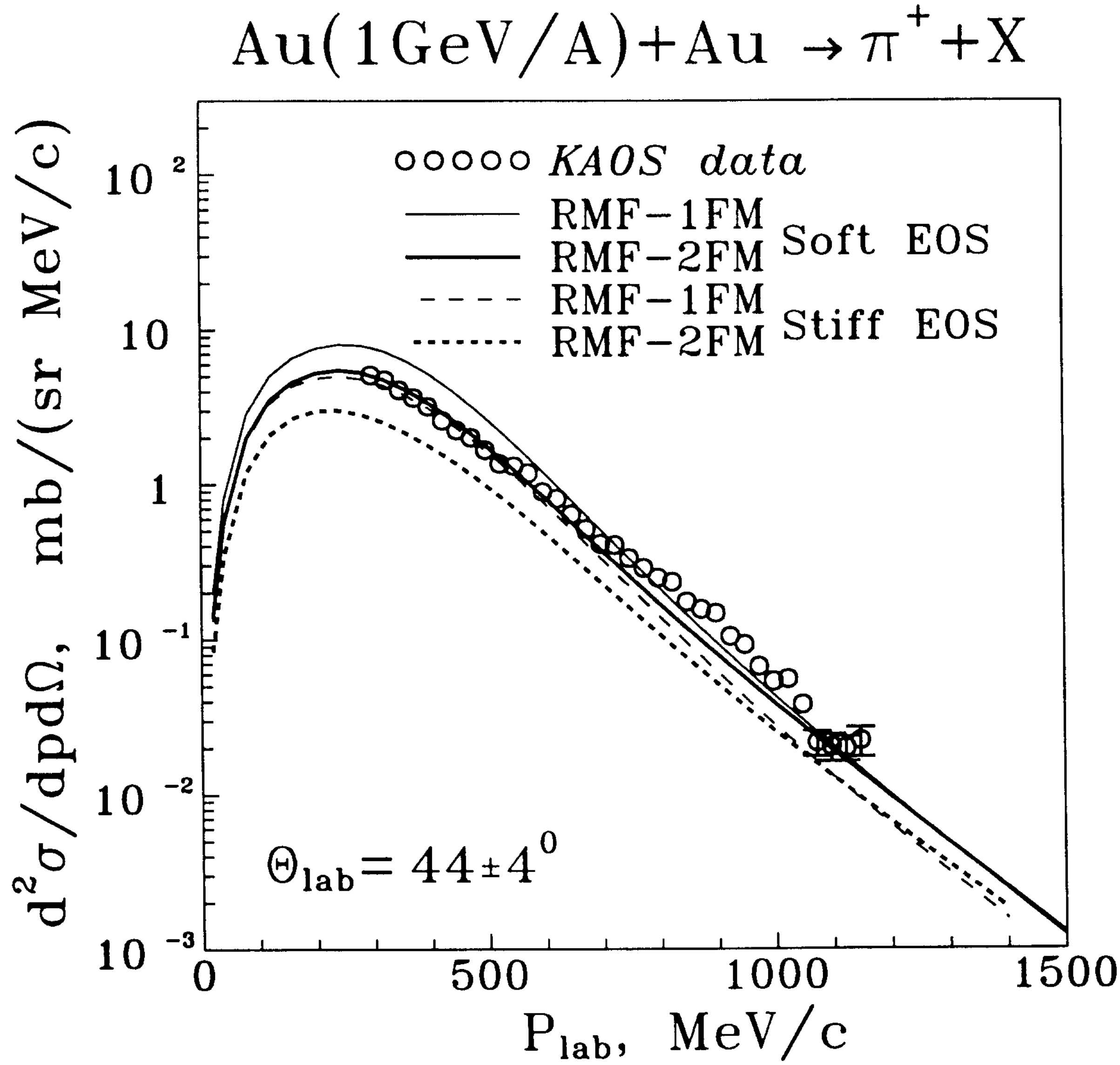
Au(1GeV/A)+Au → π⁺+X
KAOS data
RMF−1FM
RMF−2FM
Soft EOS
RMF−1FM
RMF−2FM
Stiff EOS
Θlab= 44±4°
d²σ/dpdΩ, mb/(sr MeV/c)
Plab, MeV/c
10²
10
1
10⁻¹
10⁻²
10⁻³
0
500
1000
1500

Fig. 2.

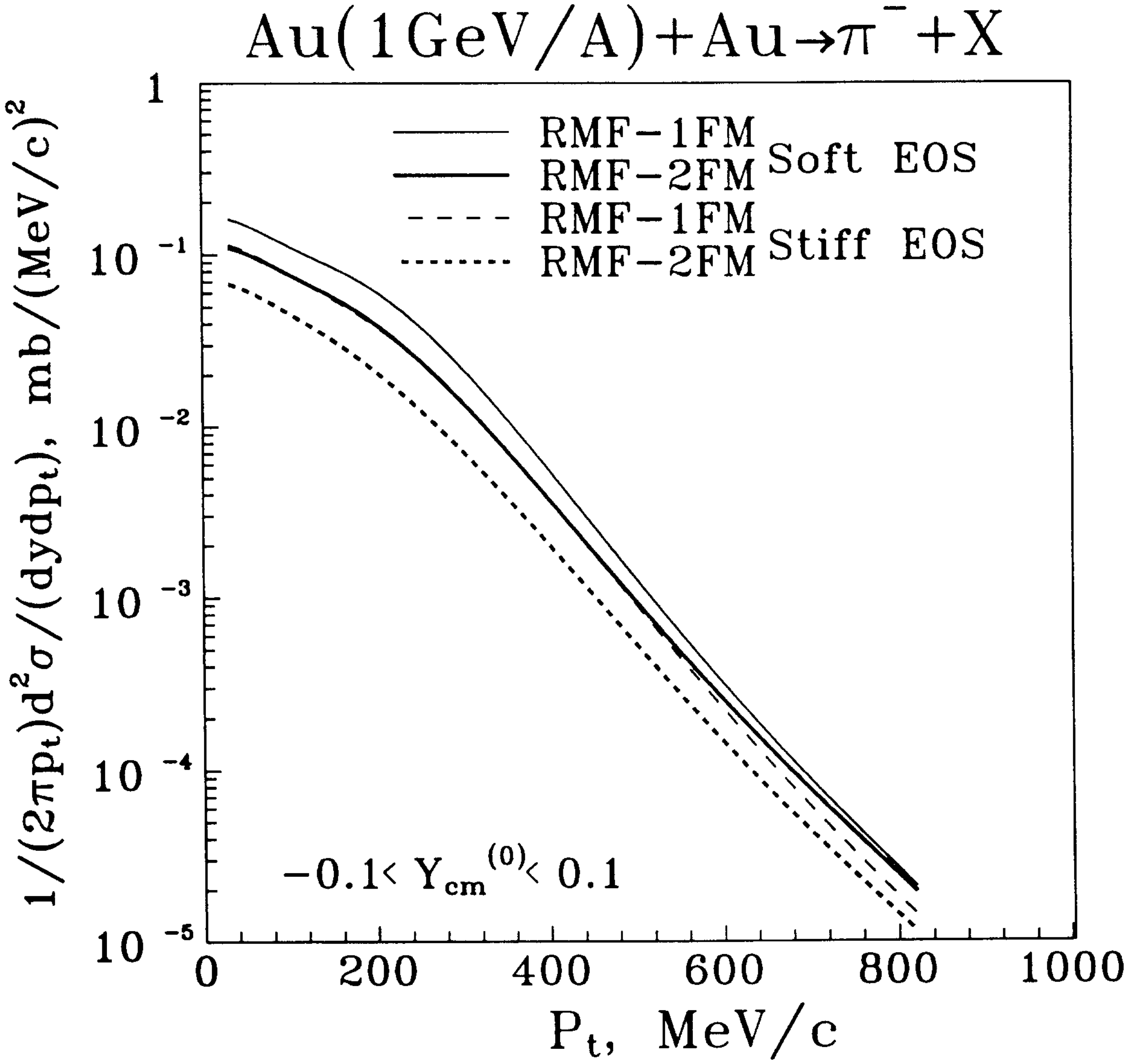
Au(1GeV/A)+Au→π⁻+X
RMF−1FM
RMF−2FM
Soft EOS
RMF−1FM
RMF−2FM
Stiff EOS
−0.1< Y_cm^(0) < 0.1
1/(2πp_t)d²σ/(dydp_t), mb/(MeV/c)²
P_t, MeV/c
1
10⁻¹
10⁻²
10⁻³
10⁻⁴
10⁻⁵
0
200
400
600
800
1000

Fig. 3.

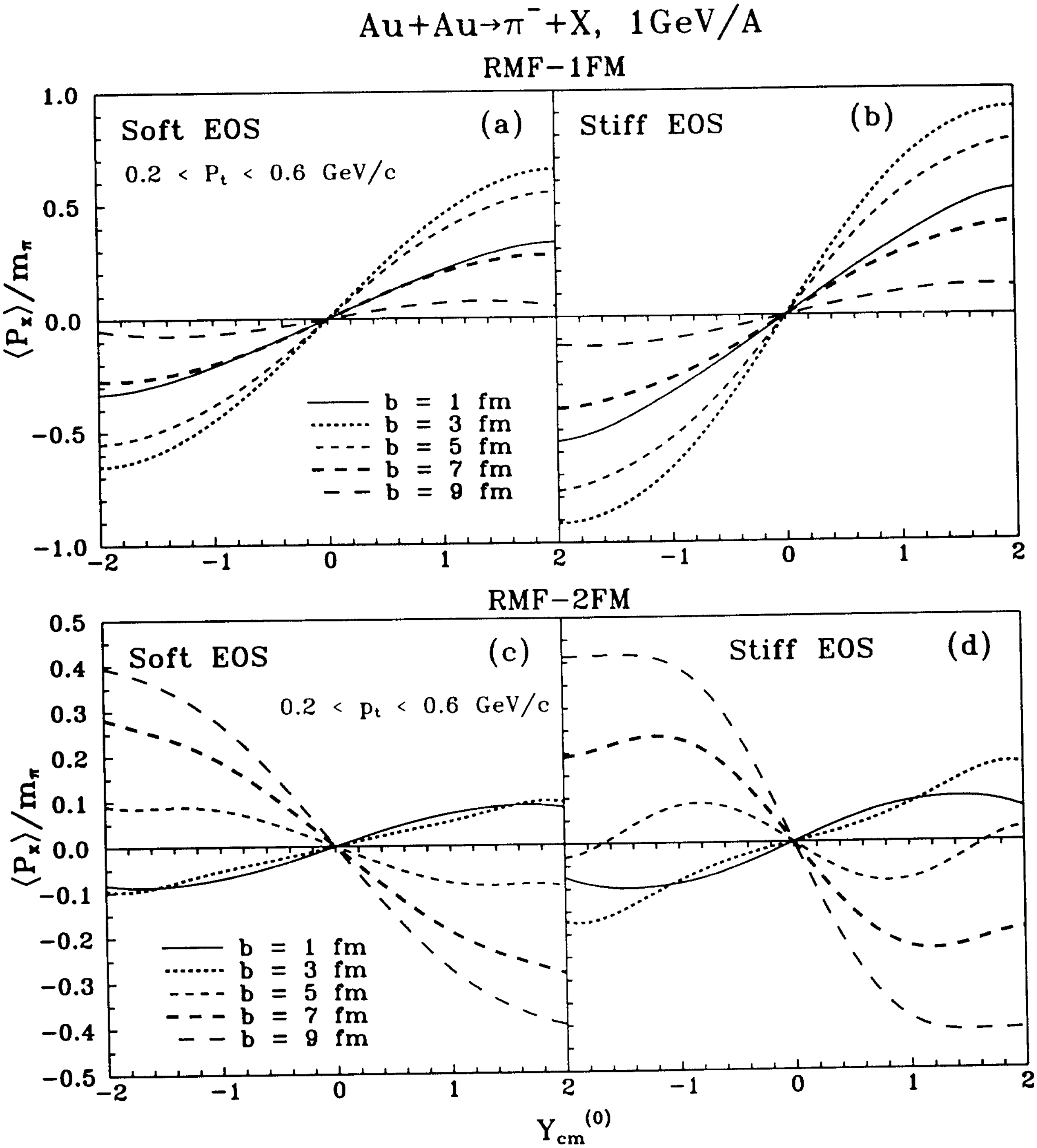
Au+Au→π⁻+X, 1GeV/A
RMF−1FM
Soft EOS
(a)
0.2 < P_t < 0.6 GeV/c
Stiff EOS
(b)
b = 1 fm
b = 3 fm
b = 5 fm
b = 7 fm
b = 9 fm
⟨P_x⟩/m_π
RMF−2FM
Soft EOS
(c)
0.2 < p_t < 0.6 GeV/c
Stiff EOS
(d)
Y_cm^(0)

Fig. 4.

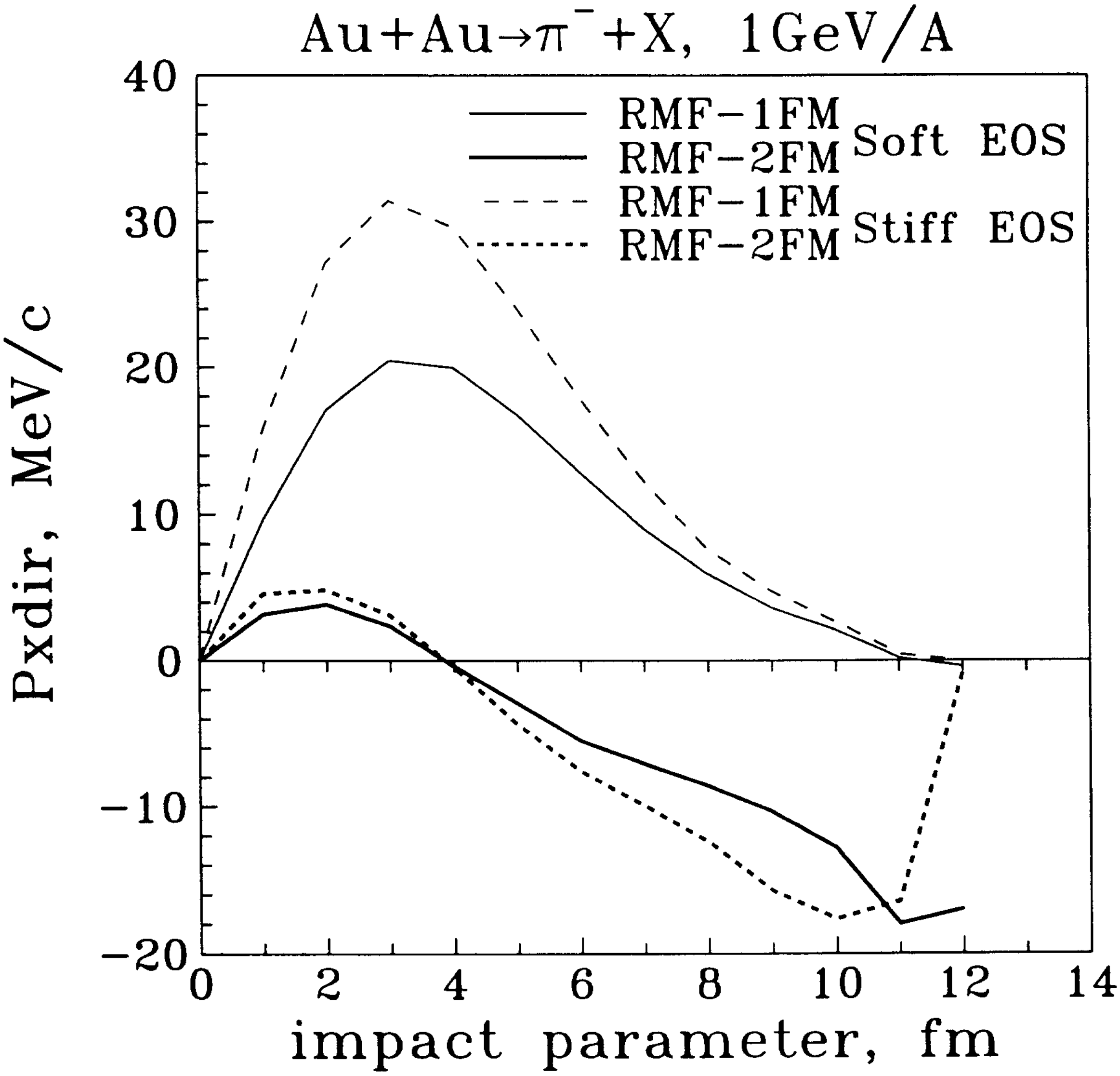
Au+Au→π⁻+X, 1GeV/A
RMF−1FM
RMF−2FM
Soft EOS
RMF−1FM
RMF−2FM
Stiff EOS
Pxdir, MeV/c
impact parameter, fm
40
30
20
10
0
−10
−20
0
2
4
6
8
10
12
14

Fig. 5.

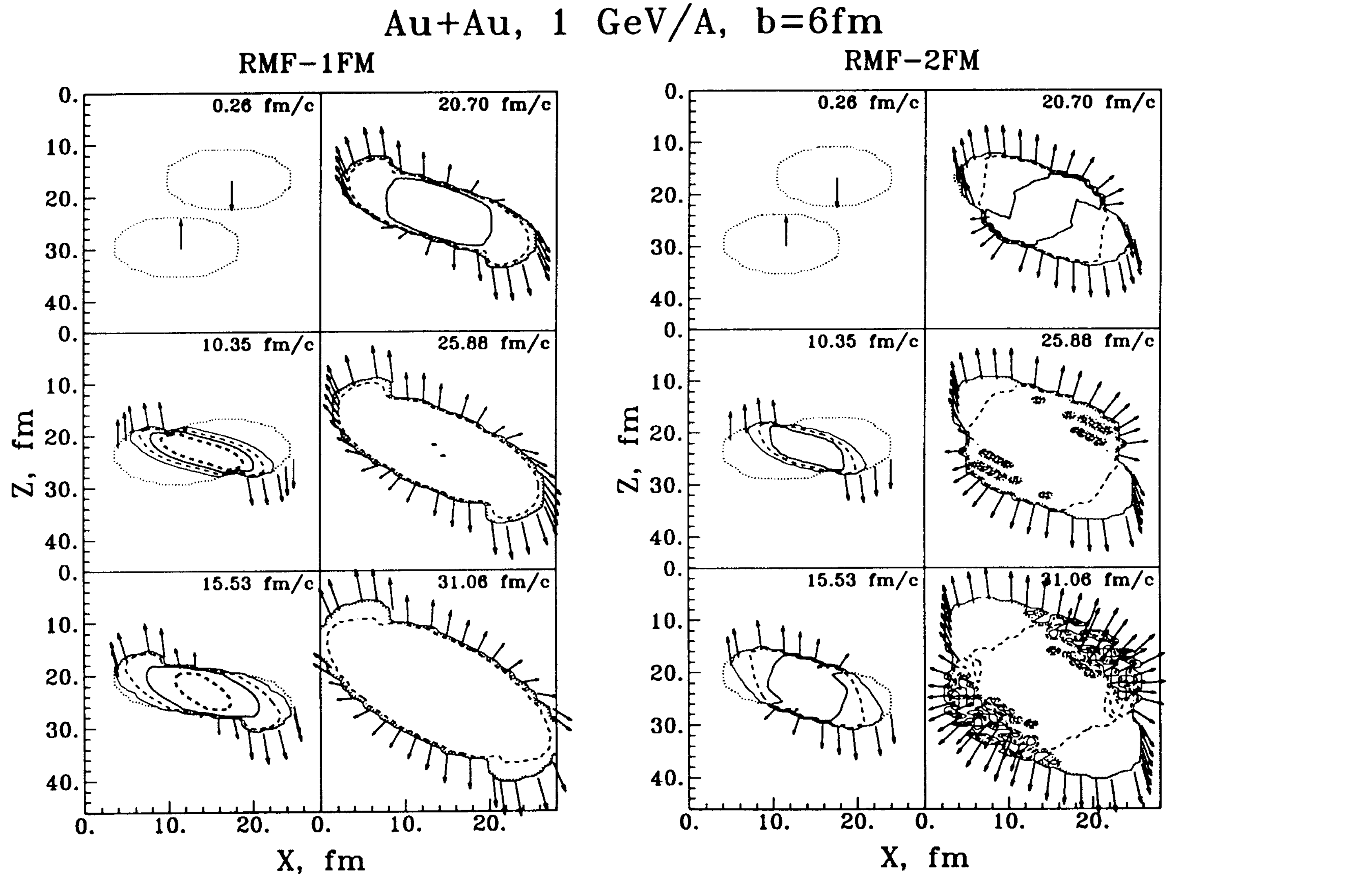
Au+Au, 1 GeV/A, b=6fm
RMF−1FM
RMF−2FM
0.26 fm/c
20.70 fm/c
10.35 fm/c
25.88 fm/c
15.53 fm/c
31.06 fm/c
Z, fm
X, fm

Fig. 6.

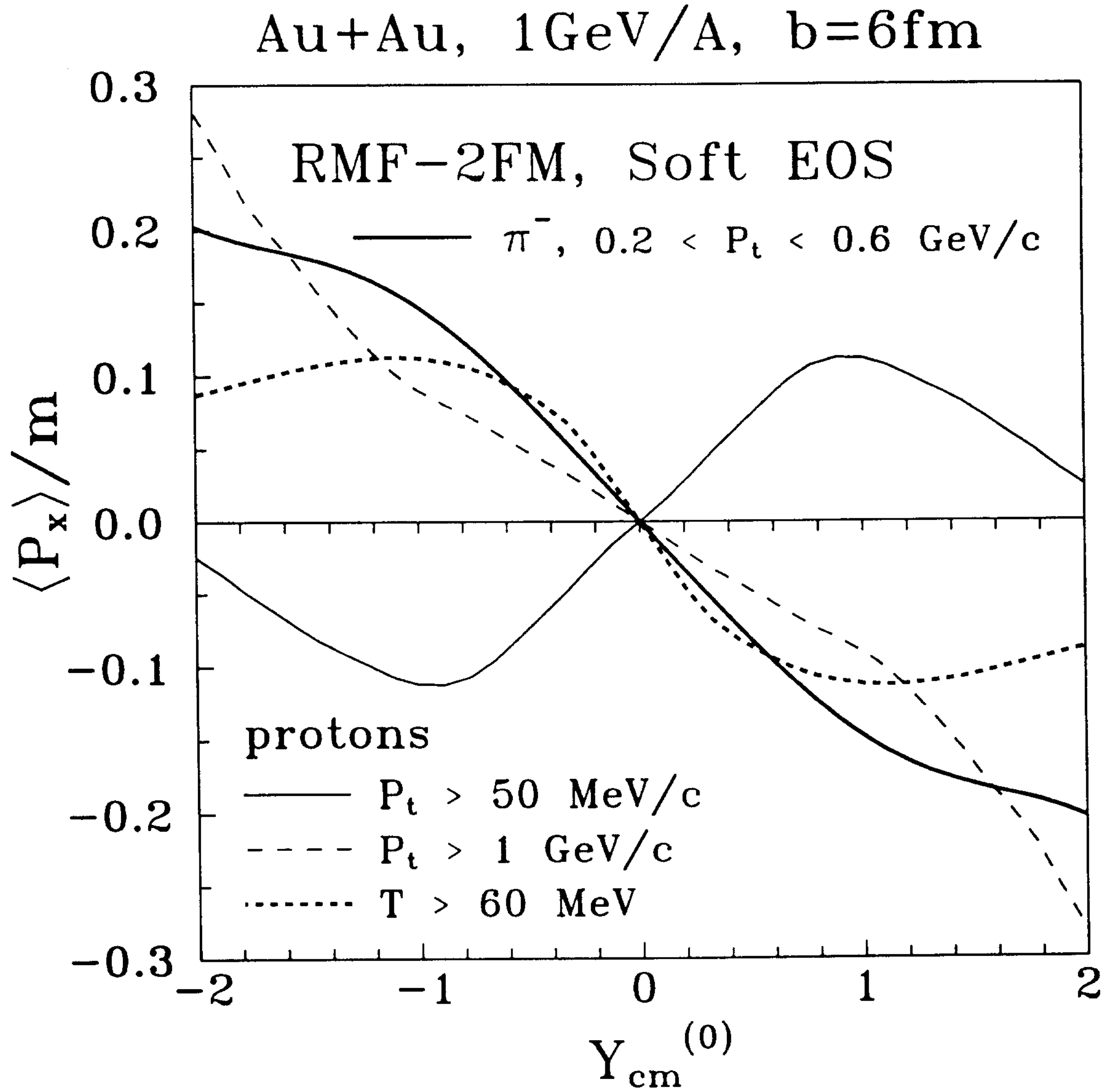
Au+Au, 1GeV/A, b=6fm
RMF−2FM, Soft EOS
π⁻, 0.2 < Pt < 0.6 GeV/c
protons
Pt > 50 MeV/c
Pt > 1 GeV/c
T > 60 MeV
⟨Px⟩/m
Ycm(0)
0.3
0.2
0.1
0.0
−0.1
−0.2
−0.3
−2
−1
0
1
2

Fig. 7.